

# RSC Advances



This is an *Accepted Manuscript*, which has been through the Royal Society of Chemistry peer review process and has been accepted for publication.

*Accepted Manuscripts* are published online shortly after acceptance, before technical editing, formatting and proof reading. Using this free service, authors can make their results available to the community, in citable form, before we publish the edited article. This *Accepted Manuscript* will be replaced by the edited, formatted and paginated article as soon as this is available.

You can find more information about *Accepted Manuscripts* in the [Information for Authors](#).

Please note that technical editing may introduce minor changes to the text and/or graphics, which may alter content. The journal's standard [Terms & Conditions](#) and the [Ethical guidelines](#) still apply. In no event shall the Royal Society of Chemistry be held responsible for any errors or omissions in this *Accepted Manuscript* or any consequences arising from the use of any information it contains.

**Synergistic interaction between POSS and fumed silica on the properties  
of crosslinked PDMS nanocomposite membranes**

Mashallah Rezakazemi<sup>1</sup>, Ali Vatani<sup>1</sup>, Toraj Mohammadi<sup>\*,2</sup>

<sup>1</sup>School of Chemical Engineering & Institute of LNG (I-LNG), Collage of Engineering,  
University of Tehran, Tehran, Iran

<sup>2</sup>Research Centre for Membrane Separation Processes, Faculty of Chemical Engineering, Iran  
University of Science and Technology (IUST), Narmak, Tehran, Iran

Corresponding author: E-mail: torajmohammadi@iust.ac.ir (T. Mohammadi); Tel: +98 21  
77240051

**Abstract**

A facile strategy for the synthesis of binary fillers nanocomposite membranes containing fumed silica (FS) and octatrimethylsiloxy polyhedral oligomeric silsesquioxane (POSS) nanoparticles was proposed to prepare high performance PDMS-FS-POSS nanocomposite membranes. To fully explore the synergistic effect between POSS and FS nanoparticles, thermal stability by thermo-gravimetric analysis (TGA) and dispersion quality by scanning electron microscopy (SEM) were investigated, while the crosslinked network was studied by Fourier transformed infrared spectroscopy (FTIR). The results showed that the thermal stability of these novel nanocomposite membranes was much better than that of the neat membrane. Thermodynamically, dipole-dipole interaction between the functional groups is the main parameter leading to better dispersion and thermal stability. Furthermore, it was found that the separation properties of different gases ( $H_2$ ,  $C_3H_8$ ,  $CO_2$  and  $CH_4$ ) across the nanocomposite membranes were enhanced with increasing FS content. All the improvements observed can be attributed to synergistic interactions between FS and POSS.

**Keywords:** Membranes, Selectivity, Mass transfer, Diffusion, Solubility.

## 1. Introduction

Separation of higher hydrocarbons ( $C_3^+$ ) from a light gas mixture traditionally requires low temperatures and expensive processes like cryogenic distillation. On the other hand, membrane separation has been recently proposed for the effective recovery of valuable hydrocarbons. The polymeric membranes for this intended application should be organic vapor selective materials such as poly(dimethylsiloxane) (PDMS) or poly(1-trimethylsilyl-1-propyne) (PTMSP). These solubility selective polymers have strong affinity with hydrocarbons enabling the separation of higher hydrocarbons from a gas mixture.

Recently, progress has been made on PDMS nanocomposite membranes preparation. PDMS membrane was selected for its excellent thermo-oxidative stability, high flexibility, low glass transition temperature ( $T_g$ ), low chemical reactivity, and low surface free energy. Although neat PDMS has excellent chain flexibility, good resistances to thermal degradation and thermo-oxidation in a wide temperature range, it still presents weak performance and cannot satisfy all the requirements for industrial application (service conditions and performances)<sup>1</sup>. To overcome these challenges, various inorganic additives have been incorporated into the polymer structure through polymerization or physical blending. It is well recognized that fumed silica (FS) is a potential candidate and has been extensively used to improve on the characteristics of PDMS membrane to meet the requirements, especially in the rubber industry<sup>2-4</sup>.

However, recent investigations tried to combine the benefits of FS and polyhedral oligomeric silsesquioxane (POSS) to prepare novel silicone based nanocomposite membranes with improved gas separation and thermal degradation resistance. Up to date, only the effects of POSS

nanoparticles on PTMSP/FS nanocomposite membrane have been investigated and Table 1 describes the most important findings from these studies.

However, PDMS, POSS and FS have similar chemical structures. POSS has a unique cage-like structure with a chemical composition of  $(\text{RSiO}_{1.5})_n$  ( $n = 6, 8, 10, \dots$ ), where R is an organic functional group, Owing to the nanosize scale of POSS and its properties, it has attracted interest in membrane studies. The most appropriate POSS for membrane is most certainly octasilsesquioxane ( $n = 8$ ) which has a cube-shaped of  $\text{Si}_8\text{O}_{12}$  cage with organic groups R at each corner. POSS nanoparticles mainly have a siloxane cage which can be tethered with a wide range of surface functional groups radiating away from the cage. The substitution of the eight trimethylsiloxy  $[-\text{OSi}(\text{CH}_3)_3]$  groups on POSS surface was found to be appropriate for our research<sup>5,6</sup>.

Until now, various types of POSS nanoparticles have been incorporated in different polymers to prepare hybrid membranes and various approaches were proposed to introduce POSS nanoparticles into the polymers: physical blending, covalent bonding with the polymer structure, and incorporation as a pendant groups on the polymer matrix<sup>7-10</sup>. The introduction of POSS nanoparticles into a polymer matrix results in enhanced membrane properties such as processability, thermal and mechanical properties, and membrane operational performance.

The unique properties of PDMS-FS and PDMS-POSS hybrid membranes have been separately investigated in several researchers, both in conceptual studies targeted at understanding the physical behavior of polymer chains in close contact with nanoparticle surfaces in response to external stimulus such as pressure, temperature, and chemical environments, as well as in applied industry. On the other hand, to the best of our knowledge, there is no related study regarding the

effect of FS on permeation and sorption properties of silicone nanocomposite membranes with POSS. However, the main purpose of this study is to investigate the effect of FS and POSS content on the resistance to thermal degradation and gas separation performance of novel silicone nanocomposite membranes. Emphasis is made on the relationships between performance (such as thermal stability and operational performance) and the nanostructure, as well as dispersion state in the nanocomposites. Furthermore, the emphasis of the current paper is on providing an account of fundamental science on the functional properties of binary systems. The incorporation of POSS and FS nanoparticles into a polymer matrix was performed through physical blending. Meanwhile, the effect of POSS and FS nanoparticles on the overall membrane structure was investigated to show how surface interactions between polymer chains and both nanofillers (as influenced by means of nanofillers surface functional groups and their contents) affect the hybrid membranes structure. The synergistic effect of POSS and FS addition on membrane performance properties such as thermal stability and nanoparticle dispersion was also explored. The 3D crosslinked structure of the PDMS based nanocomposite membranes was characterized by FTIR-ATR. It is believed that the outcomes of this study suggest valuable information and propose a roadmap for the synthesis and gas separation of POSS-related polymeric nanocomposite membranes to meet the practical requirements of commercial gas separation applications.

## **2. Experimental**

### **2.1. Materials**

To prepare PDMS-based nanocomposite membranes, DEHESIVE silicone was supplied from Wacker Silicones Corporation (USA). These materials are commonly processed in the form of a

3-component material. Each component can affect the properties of PDMS membranes. The main components are:

**Prepolymer (DEHESIVE 944):** Solvent-based addition crosslinkable PDMS (RTV 615A en B, density 1.02 g/mL, average Mw 25000, vinyl content: 0.08%) whose end group contains crosslinkable vinyl groups.

**Crosslinker V24:** hydrogen polysiloxanes (polymethylhydrogensiloxane, average Mw 2100; hydrogen content: 1.63%) with high levels of reactive Si-H groups for thermal curing of PDMS. The extent and nature of the crosslinker specifies the mechanical resistance and adhesion strength of the membrane.

**Catalyst OL:** platinum complexes (1,3-divinyl-1,1,1,3-tetramethyldisiloxane platinum (Pt) complex solution) for thermal hardening of PDMS.

The CAB-O-SIL fumed silica TS-530 (FS) with characteristic dimension of approximately 13 nm was received from Cabot Corporation Product (USA). It is well-known that FS is naturally hydrophilic due to Si-OH groups on its surface. Therefore, when directly incorporated in a hydrophobic PDMS, FS agglomeration is often encountered. The size of aggregation can be large to cause defects in the nanocomposites. However, FS has low compatibility with organic components and its surface modification by silane coupling agent has been mostly performed to improve its compatibility/dispersion in the PDMS matrix. Accordingly, the modified surface of FS was selected in this study to improve the nanoparticles compatibility with the polymer chains. Hence, TS-530 FS was selected since it has high surface area and has been surface-modified with hexamethyldisilazane. The modification substitutes hydrophilic hydroxyls on the FS surface with hydrophobic trimethylsilyl surface groups resulting in enhanced hydrophobicity. The

compatibility of the treated FS with PDMS allows faster incorporation and better dispersion than its untreated counterpart.

Nonporous crystalline octatrimethylsiloxy POSS (MS0865) nanoparticle with characteristic dimension of approximately 1.2 nm was purchased from Hybrid Plastics (USA).

The structure of the TS-530 FS and POSS nanoparticles are shown in [Figure 1](#). It can be seen that both TS-530 and POSS have the same surface functional groups. Thereby, they have similar chemical properties and compatibility with PDMS.

Toluene was of analytical purity and purchased from Anachemia Co. (Canada) and used as received. For gas separation measurements, H<sub>2</sub>, CO<sub>2</sub>, CH<sub>4</sub>, and C<sub>3</sub>H<sub>8</sub> with purity of 99.0%, 99.998%, 99.0%, and 99.0% respectively, were purchased from Praxair (Canada).

## 2.2. Nanocomposite membrane preparation

Preparation of nanocomposite membranes is noticeably complex. PDMS-FS-POSS nanocomposite membranes were synthesized through conventional solution-casting method, as the most appropriate technique to form void-free nanocomposite membranes. The flowchart of the preparation methodology for the PDMS-FS-POSS nanocomposite membranes is represented in [Figure 2](#).

The membranes formation is very sensitive to parameters such as weight proportions of silicon oil to solvent, crosslinker and the catalyst concentration, fillers moisture uptake, and evaporation time. The weight ratio of the crosslinker and the catalyst to PDMS and the synthesized conditions were kept constant, only the filler contents were changed in the formula to produce the final nanocomposite membranes.



However, pretreatment of POSS and FS nanoparticles was considered as an important parameter influencing nanocomposite membrane preparation. A more efficient moisture removal adsorbed in nanoparticles surface can be attained at high temperature. Hence, both POSS and FS nanoparticles were placed in a vacuum oven at 150°C for 24 h to remove any uptake moisture. The dried powders were then quickly cooled down to room temperature and stored in a desiccator to keep them from any organic vapors or water adsorption.

The nanocomposite membranes were prepared through physical blending of both fillers and the polymer in the solvent in the same way as to produce pristine membranes<sup>11,12</sup>. Toluene was used as the solvent for simultaneous incorporation of the fillers into the polymer chains owing to attractive fillers-solvent and PDMS-solvent interactions. The main challenge in property enhancement is the quality of fillers dispersion in the polymer matrix. This is why a sonication treatment of 10 min was carried out to break-up nanoparticle aggregation and improve homogeneity. The V24 crosslinker was subsequently introduced into the solution which was further stirred for 30 min. The catalyst was finally added and under continuous stirring for another 15 min. In the final reaction solution, the proportion of Dehesive, crosslinker and catalyst was 10:0.1:0.05 weight ratio into toluene. The reaction solution was then poured into Teflon coated glass plate and kept for curing at ambient temperature for up to 3 days. To prevent dust pollution and control evaporation rate, the casting die was covered with a glass plate. The nanocomposite membranes were dried gradually in a vacuum oven for 2 h at 80 °C to remove residual toluene and complete crosslinking reaction. It is believed that in the nanocomposites membranes, POSS produces extra crosslinking.

### 3. Membrane characterization

#### 3.1. Scanning Electron Microscopy (SEM)

Morphological observations were conducted on a JEOL JSM-840A scanning electron microscope (SEM) at a voltage of 15-20 kV.

#### 3.2. Transmission electron microscopy (TEM)

TEM images were taken using a Philips Tecnai 20 at an accelerating voltage of 200 kV.

#### 3.3. Fourier transform infrared spectroscopy (FTIR)

FTIR is extensively used to evaluate the chemical property of nanocomposite membranes including chemical bonds, molecular energy levels, molecular orientations, and molecular interactions. FTIR was performed on the membranes as well as the nanoparticles using a Nicolet Magna 850 Fourier transform infrared spectrometer (Thermo Scientific, Madison, WI). All samples were dried in a vacuum oven prior to measurement to remove water. The IR spectra were obtained continuously in the 3600-400  $\text{cm}^{-1}$  wavenumber range at a resolution of 4  $\text{cm}^{-1}$  using Happ-Genzel apodization. Attenuated total reflectance (ATR) method was used to collect the membrane spectra with the FTIR apparatus equipped with a liquid-nitrogen cooled narrow-band mercury/cadmium/telluride (MCT) detector using Golden-Gate (diamond IRE) ATR accessories (Specac Ltd., UK). Suitable background corrections were also performed.

### 3.4. Thermogravimetric Analysis (TGA)

TA Instruments thermogravimetric analyzer (TGA), model Q5000IR, was used to fully investigate thermal analysis of FS and POSS nanoparticles as well as PDMS-FS-POSS nanocomposite membranes. The onset of decomposition temperature ( $T_{onset}$ ) was determined through the weight percent versus temperature curve. The study proposes the use of the derivative thermogravimetric curve (DTG) to analytically explain the nature of degradation realized in either both nanoparticles or in nanocomposites. A constant rise of temperature (10 °C/min up to 950 °C) under controlled nitrogen environment was implied for all the membranes. A fine nanoparticle of 5 to 10 mg was packed cautiously into the pan to form a uniform layer. The PDMS and PDMS-FS-POSS (10 to 16 mg) nanocomposite films were cut into small rectangular pieces and housed in the pan. Dry nitrogen inert gas flowing over the balance (10 ml/min) and the sample chamber (25 ml/min).

## 4. Results and discussion

### 4.1. Morphology of PDMS-FS-POSS nanocomposite membranes

There are numerous important challenges faced in synthesizing POSS-based nanocomposite membranes such as nanoparticles dispersion, processability, durability, thermostability, oxidation and reliability which are major issues for large-scale production.

Morphological analysis of an inorganic-organic nanocomposite membrane can provide valuable information on uniformity and distribution of the nanoparticles in a polymer matrix. For instance, in the case of nanoscale inorganic additives, phase separation and agglomeration can be observed by SEM and TEM images. The representative SEM photographs from the cross-

sections of PDMS-POSS 2%-FS 5%, PDMS-POSS 2%-FS 10% and PDMS-POSS 2%-FS 15% are respectively shown in [Figure 3](#) which reveals that uniform distribution of both FS and POSS within the PDMS matrix was achieved without any voids/defects at the polymer-filler interfaces. TEM images in [Figure 4](#) also reveal the well-defined nanometer scale distribution of fillers.

The dispersability and easy handling of POSS in an organic solvent and therefore polymer matrix is a main challenge to get well dispersed POSS in hybrid membranes synthesized by conventional physical blending. The lack of strong attraction between POSS nanoparticles allows good filler dispersion in the polymer matrix. Also, surface functional groups provide a pathway where the surface chemistry of POSS can improve its stable dispersion in the polymer matrix.

However, it can be speculated for the compatibility of the octatrimethylsiloxy POSS with PDMS-FS nanocomposite structure is owed to high dipole-dipole interactions between the functional groups and polymer. Nanoparticles comprising similar surface properties as the polymer exhibit better adhesion with the polymer. This results in better contact of the nanoparticles with the polymer as well as better distribution. The larger the difference of the surface energies of polymer and nanoparticles, the higher is the thermodynamic driving force of the nanoparticles to agglomerate. Hence, a modified nanoparticles surface can prevent nanoparticles agglomeration in the polymer structure. On the basis of molecular dynamics simulation, Striolo et al.<sup>13</sup> explored the thermodynamic and transport properties of octamethyl and octahydro substituted POSS incorporated into PDMS. The findings revealed that POSS nanoparticles do not have a tendency to adsorb on each other when incorporated in PDMS. When the relative interaction to POSS-POSS is favorable, POSS nanoparticles is well dispersed and the physical properties of the nanocomposite systems are directly related to the POSS dispersion level.

Polymers interact with both fillers by van der Waals and dipole-dipole interactions, resulting in better stable dispersion of FS and POSS in specific organic solvents and matrices. The main difference is when the POSS content increases, FS nanoparticles dispersion became somewhat better as seen in [Figure 3](#). This decreases the inter-nanoparticle forces and helps dispersion. POSS was chosen for its chemistry leading to strong attachment to the nanoparticles and organic groups that are compatible with the surrounding matrix. Therefore, POSS is helpful in controlling nanoparticles dispersion in polymer membranes via cooperative surface interactions. The homogeneous distribution of both FS and POSS nanoparticles within the polymer matrix depends on the cooperative surface interactions of POSS functional groups through van der Waals force and polarity with the polymer. Octatrimethylsiloxy substituted POSS has high hydrophobicity due to its trimethylsiloxy groups. POSS compounded in the PDMS improves the structure of the nanocomposites and change permeant diffusion through the nanocomposite membranes. As a matter of fact, when POSS is used as fillers in PDMS, it affects the polymer chains motion within the nanocomposite membranes. It is believed that POSS distribution in the nanocomposite prevents the molecular motion of the polymer chains whereby gas permeation changes.

Moreover, there was an inevitable trade-off between both POSS and FS nanoparticle loadings. As seen in [Figure 3](#), POSS dispersion became better with increasing FS content while increasing the total amount of nanofillers in the PDMS matrix leads to nanofillers agglomeration.

#### 4.2. FTIR characterization

The FTIR spectra were used to explore the structure-property relationship of the PDMS-FS-POSS nanocomposite membranes. Figure 5 presents the spectra of the neat PDMS and both virgin fillers, as well as the different PDMS-FS-POSS nanocomposite membranes. ATR-IR spectra for the neat POSS exhibited a strong peak at  $1060\text{ cm}^{-1}$  associated to symmetric Si–O–Si stretching, thus confirming the silsesquioxane cages.

All the PDMS-FS-POSS hybrid membranes have similar FTIR spectra as compared to that of the reference membrane. The functional groups on the surface of POSS and FS facilitates synergistic effects between both nanoparticles was improved by hydrogen bonds, and van der Waals force<sup>7, 8, 14</sup>. Numerous crosslinked 3D networks were produced during crosslinking and thermal processing. The crosslinked networks of the PDMS nanocomposite membranes were studied by FTIR analysis. All hybrid membranes display virtually identical spectra, as presented in Figure 5. However, a peak at  $790\text{ cm}^{-1}$  is attributed to  $-\text{CH}_3$  rocking and  $-\text{Si}-\text{C}-$  stretching in  $-\text{Si}-\text{CH}_3$ . The bands at  $900\text{ cm}^{-1}$ ,  $1258\text{ cm}^{-1}$ ,  $1455\text{ cm}^{-1}$  and  $2960\text{ cm}^{-1}$  are assigned to  $-\text{Si}-\text{O}$  stretching in  $-\text{Si}-\text{OH}$ , symmetric  $-\text{CH}_3$  deformation in  $-\text{Si}-\text{CH}_3$ , C–H bending and  $-\text{CH}_2-$  stretching in  $-\text{Si}-\text{CH}_2-$ , respectively. Moreover, the bands at  $1060\text{ cm}^{-1}$  and  $1005\text{ cm}^{-1}$  are related to the Si–O–Si stretching vibration of the crosslinked PDMS in these novel nanocomposite membranes. The presence of the Si–O–Si stretching absorption peak in the nanocomposite membranes indicates that POSS is well incorporated into the PDMS molecular chains. The intensity of these bands further increases with POSS content in the nanocomposite membranes.

#### 4.3. Thermal stability of the PDMS-FS-POSS nanocomposite membranes

One major application of TGA is the assessment of thermal stabilities of the fillers contents in polymers and nanocomposites. The morphology and nanofiller functionality plays a vital role in

thermal stability of the nanocomposite membranes. However, there have been numerous studies focusing on thermal stability of POSS-containing polymer nanocomposites by TGA <sup>5, 6, 9, 15, 16</sup>.

Figure 6 shows the TGA and DTG curves of FS and POSS nanoparticles in nitrogen. Within a temperature range of 200-300 °C, POSS is rapidly decomposed with almost complete weight loss which can be associated to the sublimation of octatrimethylsiloxy groups. Hence, POSS itself cannot exhibit thermal stability in nitrogen. On the other hand, only 10.6% weight loss was observed for FS nanoparticles up to 900 °C showing that FS nanoparticles have better thermal stability than POSS.

Figure 7 shows TGA results of the PDMS-POSS nanocomposite membranes. It is clear that PDMS thermal stability increases with increasing POSS content. This can be related to the interactions and the tight Si–O frameworks <sup>7, 10, 17</sup>. This indicates that the intramolecular dipole-dipole interactions between the octatrimethylsiloxy groups improve thermal stability of the nanocomposites <sup>7, 10, 17</sup>.

DTG results in Figure 8 show that there is only one degradation step in thermal decomposition of all the samples. POSS has a rapid thermal degradation starting around 250 °C, while the membranes have slower thermal degradation over a wider range of temperature where the starting decomposition temperature increases with increasing the POSS content. This reveals that the combination of POSS with PDMS alters thermal stability of the membranes and indicates that incorporation of octatrimethylsiloxy POSS is effective to enhance thermal stability of these nanocomposite membranes. However, the PDMS-POSS nanocomposite membrane with 6% wt. POSS exhibits the highest thermal stability with a decomposition range at 500-700 °C, which may be attributed to the strong bonding between PDMS chains and POSS nanoparticles.

In the inert nitrogen environment, the thermodegradation profiles of the PDMS-based nanocomposites membranes composed of FS and POSS nanoparticles were also assessed by TGA, and their behaviors are shown in [Figures 9-11](#). On the basis of the TGA-DTG results, it can be concluded that all of the PDMS-FS-POSS nanocomposite membranes presented two degradation steps in DTG curves. The first decomposition peak is around 440-475 °C, while the second one is around 680-750 °C, but most of the decomposition occurred at the higher temperature.

PDMS however has a tendency to decompose into cyclic trimers and tetramers at high temperature as a result of thermodynamic ring-chain equilibrium through the nanocomposites structures, and this equilibrium is limited when an inorganic filler is introduced in the host matrix [18](#).

The resistance to thermal decomposition of the PDMS-FS-POSS nanocomposite membranes was significantly enhanced by introducing FS and POSS nanoparticles. This noticeable improvement was contributed to the increased interaction of the host polymer chains and fillers caused by synergistic effect between FS and POSS nanoparticles. This is also may be associated to the intrinsically high thermal stability of the FS which is higher than 420 °C when embedded into stable PDMS-POSS membranes enhanced their thermostability by increasing PDMS-fillers interactions and the tight inorganic Si–O frameworks [10](#). Hence, thermally stable bonding occurs among the inorganic and organic components and the influence of the thermally stable inorganic Si–O networks on the thermal property of hybrid membranes was significant at elevated temperatures. From screening the results, however, it can be deduced that octatrimethylsiloxy POSS and FS have a profound enhancement on the thermal property of PDMS-based



nanocomposite membranes. Therefore, PDMS-FS-POSS nanocomposite membranes can act an imperative role in high-temperature applications <sup>10</sup>.

Consequently, in point of fact, three reasons can be considered for successful to achieve these experimental results on thermal stability of nanocomposite membranes: I) the homogenous distribution of the crosslinked 3D structures originating from synergistic effect between the POSS and FS can develop the resistance of the PDMS membrane to thermal degradation; II) the vinyl groups in PDMS could easily crosslink at low temperature when the PDMS membranes thermally degraded, that create the crosslinked 3D structures more rigid; III) the rigid 3D structures could more hinder random motions of the polymer chains, and prevent the creation of degrading yields, that could enhance thermal stability of the loaded PDMS-FS-POSS nanocomposite membranes. The most effect could be the competitive results of the three aforementioned reasons <sup>7, 8, 14, 17, 19-21</sup>. When the fillers content in binary system is high, the combined action of the homogenous distribution of the crosslinked 3D structures and the vinyl groups in these PDMS-FS-POSS nanocomposite membranes dominate during the thermal decomposition process.

Finally, in accordance with the discussion presented above, it can be concluded that when the fillers content enlarges further synergistic effect between FS and POSS is observed, and distribution of FS and POSS becomes uniform, which also results in resistance to degradation of the PDMS-FS-POSS nanocomposite membranes as well.

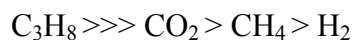
Zhang et al. <sup>5</sup> studied PDMS with octamethyl substituted POSS and tetraethoxysilanes/dibutyltin dilaurate, while Liu et al. <sup>22</sup> studied POSS grafted room temperature vulcanized (RTV-g-POSS) presented similar degradation trends for POSS-containing nanocomposite membranes. Hong et

al.<sup>23</sup>, Beltran et al.<sup>3</sup>, Nisola et al.<sup>24</sup>, and Song et al.<sup>2</sup> also found a similar thermal degradation for silica containing nanocomposite membranes. For binary nanocomposite films, Chen et al.<sup>14</sup>,<sup>19</sup> reported a similar thermal degradation for octa[(trimethoxysilyl)ethyl]-POSS and room temperature vulcanized (RTV) silicone rubbers.

#### 4.4. Effect of pressure and fillers content on gas permeation

The detailed description of the gas permeation procedure can be found elsewhere as in our previous study<sup>25</sup>. Figure 12 shows permeability coefficient of H<sub>2</sub>, C<sub>3</sub>H<sub>8</sub>, CO<sub>2</sub> and CH<sub>4</sub> at 35°C as a function of FS nanoparticles concentration within the PDMS-POSS 2 wt.% matrix at different operating pressures. The results of binary nanofillers (POSS and FS) into PDMS nanocomposites on gas permeation were clearly observed.

Figure 12 illustrates the effect of FS nanoparticles fillings on the permeation coefficient of the PDMS-POSS nanocomposite membranes. As observed, the permeability of CO<sub>2</sub> and C<sub>3</sub>H<sub>8</sub> across the PDMS-FS-POSS nanocomposites enhances with enhancing feed pressure while for H<sub>2</sub> and CH<sub>4</sub> decreases but pressure has minor effect on H<sub>2</sub> and CH<sub>4</sub> permeability. The increment in permeabilities with pressure for CO<sub>2</sub> and C<sub>3</sub>H<sub>8</sub> through the PDMS-FS-POSS nanocomposites was more profound than H<sub>2</sub> and CH<sub>4</sub>. This trend clearly indicates that the tortuous routes of species penetration and the polymer compactness may affected transport properties. The arrangement of permeability coefficient through the PDMS-FS-POSS nanocomposite membranes is as follows:



The results have ascertained that the employment of the FS into the PDMS-POSS polymer matrix increase  $C_3H_8$  and  $CO_2$  permeability. Indeed, the nanocomposites performance is changes due to the permeating molecules when the polymeric membrane is filled with nanofillers. The nature of the permeating molecules-polymer interaction has a significant effect on the nanofillers-polymer interface. From screening gas permeation data, it can be deduced that in the presence of  $C_3H_8$  and  $CO_2$ , a favorable interaction between polymer and functional group of nanofillers in the nanocomposites occurs. The functional groups in the nanocomposite structure can interact with the polymer chains and the gas molecules, and trimethylsiloxy groups at apex silicone atoms enhanced hydrophobicity of the nanoparticles. However, one possibility reason for this enhancement can be pointed to the  $C_3H_8$  and  $CO_2$  molecules adsorption at the nanofillers-PDMS interfaces and also at the external surfaces of the fillers nanoparticles and this provide a driving force for the  $C_3H_8$  and  $CO_2$  molecules leading to develop the nanocomposites permeability. Consequently, the trimethylsiloxy functional groups have some interactions with permanent gaseous which facilitate their permeation through the nanocomposites.

Higher feed flow pressure, and thus, enhancing permeant concentration in polymer, the membrane affinity to plasticization increases, particularly for highly condensable gases. Imposed higher pressure on the nanocomposites surface could gradually compact the polymer matrix. Further to these dual effects that increases diffusivity, solubility often enhances with increase in feed pressure, predominantly for more soluble species, leading to higher permeability coefficient

26

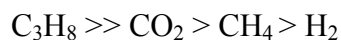
Without a doubt, the more condensable gases have substantial result on plasticization of elastomeric membranes, and this effect for the nanocomposites can be also seen. Since operating pressure rises, the plasticization, as respect to the more condensable gases, intensifies; so that,

the gas sorption in the polymer domain. Therefore, the gas transport of more condensable components such as  $C_3H_8$  and  $CO_2$  rises at high pressure, whereas for less condensable gases such as  $H_2$  or  $CH_4$  decreases.

An overall downward trend of permeability for  $H_2$  and  $CH_4$  gases with an increment in FS composition was observed in [Figure 12](#).  $H_2$  showed a 20.98% reduction in permeability coefficient as the FS loadings enhanced from 0 to 15 wt.% at 8 bar.  $CH_4$  also exhibited a continuous reduction in permeation from 0 to 15 wt.% FS composition at 8 bar. The PDMS-POSS 2 wt.%-FS 15 wt.% nanocomposite membrane exhibited a 21.01% reduction in  $CH_4$  permeation. The nanofillers loading have major effect than pressure on  $H_2$  and  $CH_4$  permeability. The incorporation of 15 wt.% nano-FS particles increases the permeation of  $C_3H_8$  and  $CO_2$  at 8 bar in PDMS-POSS-FS nanocomposites closely 26% and 6%, respectively.

#### 4.5. Effect of pressure and fillers content on gas concentration

The detailed description of the gas sorption procedure can be found elsewhere as in our previous study <sup>27</sup>. The solubility of  $CO_2$ ,  $CH_4$ ,  $H_2$ , and  $C_3H_8$  in all PDMS-FS-POSS nanocomposite membranes with various FS loading at 35 °C is represented in [Figure 13](#). According to experimental results presented here, the sequence of concentration of gases in the neat film is as



which is in close agreement with their  $T_c$  values. In a series of gases,  $T_c$  roughly increases as penetrant size increases, and therefore sorption enhances as the penetrant size increases.

On the basis of experimental results, it can be deduced that the penetrant sorption improves in the sequence of PDMS < PDMS-FS (5 < 10 < 15 wt.%) - POSS 2 wt.%. The order of sorption isotherms are in accord with increasing FS loading. This is possibly can be attributed to the solubility of gases in the surface of nanofillers; thereby, it may improve sorption capacity of the nanocomposites. Therefore, the higher solubility capacities are mainly due to the additional sorptive site provided by extra nanofillers content. The solubility of CO<sub>2</sub>, CH<sub>4</sub> and H<sub>2</sub> are almost constant in the pristine and the PDMS-FS-POSS 2 wt.% nanocomposites while the C<sub>3</sub>H<sub>8</sub> solubility in all the prepared nanocomposites increases with pressure.

## 5. Conclusion

The nanoparticles of POSS and FS were introduced into the PDMS to fully explore the potential property-improving effects that nanofillers have been shown to have on silicon polymer in intended gas separation applications. POSS nanoparticles have proposed effective for formulation nanocomposite membranes having specialty binary nanofillers incorporated into PDMS polymer system. The nanocomposite membranes containing binary additives show synergism in the physicochemical properties such as dispersion and thermal stability. SEM images exhibited that the nanosized FS and POSS were homogeneously distributed in the polymer structure indicating that trimethylsiloxy functional groups on the surface of FS and POSS nanosphere are compatible with the PDMS matrix. It can be speculated for the compatibility of the octatrimethylsiloxy POSS with PDMS-FS nanocomposite structure is owing to the high dipole-dipole interaction between the functional groups. Hence, appropriate surface-functionalized nanosized FS and POSS nanoparticles were recognized for PDMS membrane. The experimental results obtained from TGA investigations indicate that the PDMS-FS-POSS

nanocomposite membranes present better thermal stability due to the presence of Si-O networks in the structure. Moreover, the gas permeation results also indicated that the PDMS-FS-POSS nanocomposite membrane is very promising for  $C_3H_8/H_2$ ,  $C_3H_8/CO_2$  and  $C_3H_8/CH_4$  separation and separation properties were enhanced with the increment of the content of nano-FS.

## References

- 1 M. Rezakazemi, K. Shahidi and T. Mohammadi, *Desalination and Water Treatment*, **2014**, 1.
- 2 Y. Song, J. Yu, D. Dai, L. Song and N. Jiang, *Materials & Design*, **64**, **2014**, 687.
- 3 A.B. Beltran, G.M. Nisola, E. Cho, E.E.D. Lee and W.-J. Chung, *Appl. Surf. Sci.*, **258**, **2011**, 337.
- 4 M. Rezakazemi, A. Ebadi Amooghin, M.M. Montazer-Rahmati, A.F. Ismail and T. Matsuura, *Prog. Polym. Sci.*, **39**, **2014**, 817.
- 5 Q.G. Zhang, B.C. Fan, Q.L. Liu, A.M. Zhu and F.F. Shi, *J. Membr. Sci.*, **366**, **2011**, 335.
- 6 Y. Meng, Z. Wei, L. Liu, L. Liu, L. Zhang, T. Nishi and K. Ito, *Polymer*, **54**, **2013**, 3055.
- 7 D. Chen, Y. Liu and C. Huang, *Polym. Degrad. Stab.*, **97**, **2012**, 308.
- 8 D. Chen, S. Yi, W. Wu, Y. Zhong, J. Liao, C. Huang and W. Shi, *Polymer*, **51**, **2010**, 3867.
- 9 D. Yang, W. Zhang, R. Yao and B. Jiang, *Polym. Degrad. Stab.*, **98**, **2013**, 109.
- 10 D. Zhang, Y. Liu, Y. Shi and G. Huang, *RSC Advances*, **4**, **2014**, 6275.
- 11 M. Rostamizadeh, M. Rezakazemi, K. Shahidi and T. Mohammadi, *Int. J. Hydrogen Energy*, **38**, **2013**, 1128.
- 12 M. Rezakazemi and T. Mohammadi, *Int. J. Hydrogen Energy*, **38**, **2013**, 14035.
- 13 A. Striolo, C. McCabe and P.T. Cummings, *The Journal of Physical Chemistry B*, **109**, **2005**, 14300.

- 14 D. Chen, S. Yi, P. Fang, Y. Zhong, C. Huang and X. Wu, *Reactive and Functional Polymers*, 71, **2011**, 502.
- 15 M.L. Chua, L. Shao, B.T. Low, Y. Xiao and T.-S. Chung, *J. Membr. Sci.*, 385–386, **2011**, 40.
- 16 B. Dasgupta, S.K. Sen and S. Banerjee, *Materials Science and Engineering: B*, 168, **2010**, 30.
- 17 D. Chen, C. Huang and X. Hu, *Polym. Compos.*, 34, **2013**, 1041.
- 18 R.A. Rhein, in, Naval Weapons Center China Lake, California 93555, **1983**.
- 19 D. Chen, J. Nie, S. Yi, W. Wu, Y. Zhong, J. Liao and C. Huang, *Polym. Degrad. Stab.*, 95, **2010**, 618.
- 20 D. Chen, Y. Liu, H. Zhang, Y. Zhou, C. Huang and C. Xiong, *J. Inorg. Organomet. Polym. Mater.*, 23, **2013**, 1375.
- 21 Y. Zhang, Y. Mao, D. Chen, W. Wu, S. Yi, S. Mo and C. Huang, *Polym. Degrad. Stab.*, 98, **2013**, 916.
- 22 Y. Liu, Y. Shi, D. Zhang, J. Li and G. Huang, *Polymer*, 54, **2013**, 6140.
- 23 H. Hong, L. Chen, Q. Zhang and Z. Zhang, *Polym. Eng. Sci.*, 51, **2011**, 819.
- 24 G. Nisola, A. Beltran, D. Sim, D. Lee, B. Jung and W.-J. Chung, *J. Polym. Res.*, 18, **2011**, 2415.
- 25 M. Reza kazemi, K. Shahidi and T. Mohammadi, *Int. J. Hydrogen Energy*, 37, **2012**, 14576.
- 26 A. Singh, B.D. Freeman and I. Pinnau, *J. Polym. Sci., Part B: Polym. Phys*, 36, **1998**, 289.



27 M. Rezakazemi, K. Shahidi and T. Mohammadi, *Int. J. Hydrogen Energy*, 37, **2012**, 17275.

28 W.A. Reinerth, J.J. Schwab, J.D. Lichtenhan, Q. Liu, D. Hilton, B.D. Freeman, L. Toy and H.J. Lee, *Abstracts of Papers, 222<sup>nd</sup> ACS National Meeting (MTLS-020), Chicago, IL, United States*, **2001**.

29 S.D. Kelman, B.W. Rowe, C.W. Bielawski, S.J. Pas, A.J. Hill, D.R. Paul and B.D. Freeman, *J. Membr. Sci.*, 320, **2008**, 123.

30 S.D. Kelman, in: PhD Dissertation, The University of Texas at Austin **2008**.

31 H. Lin, B. Freeman, L. Toy, T. Merkel and R. Gupta, in: 2003 DOE University Coal Research Contractors' Meeting, Available online at: [www.netl.doe.gov/publications/proceedings/03/ucr-hbcu/Freeman.pdf](http://www.netl.doe.gov/publications/proceedings/03/ucr-hbcu/Freeman.pdf), **2003**.

## Figures Caption

Figure 1. The chemical structure of: a) surface treated hydrophobic TS 530 FS and b) POSS MS0865.

Figure 2. Processing flowchart for the PDMS-FS-POSS nanocomposite membranes.

Figure 3. Cross-sectional SEM images of: (a) PDMS-POSS 2%-FS 5%, (b) PDMS-POSS 2%-FS 10%, and (c) PDMS-POSS 2%-FS 15% nanocomposite membranes.

Figure 4. TEM images of PDMS-POSS 2%-FS 10% nanocomposite membranes.

Figure 5. FTIR-ATR spectra for FS and POSS nanoparticles, neat PDMS, and PDMS-FS-POSS nanocomposite membranes.

Figure 6. TGA-DTG curves for FS and POSS nanoparticles obtained in a nitrogen atmosphere.

Figure 7. TGA curves for neat PDMS and PDMS-POSS nanocomposite membranes obtained in nitrogen atmosphere.

Figure 8. DTG curves for PDMS and PDMS-POSS nanocomposite membranes obtained in nitrogen atmosphere.

Figure 9. TGA-DTG curves of PDMS-FS-POSS nanocomposite membranes obtained in a nitrogen atmosphere at FS 5 wt.% and various POSS contents.

Figure 10. TGA-DTG curves of PDMS-FS-POSS nanocomposite membranes obtained in a nitrogen atmosphere at FS 10 wt.% and various POSS contents.

Figure 11. TGA-DTG curves of PDMS-FS-POSS nanocomposite membranes obtained in a nitrogen atmosphere at FS 15 wt.% and various POSS contents.

Figure 12. Permeability of the penetrants ( $H_2$ ,  $CO_2$ ,  $CH_4$  and  $C_3H_8$ ) through the synthesized PDMS-FS-POSS nanocomposite membranes as a function of feed pressure and FS nanoparticles weight content.

Figure 13. Penetrants concentration ( $H_2$ ,  $CO_2$ ,  $CH_4$  and  $C_3H_8$ ) in the synthesized PDMS-FS-POSS nanocomposite membranes as functions of feed pressure and FS nanoparticles weight content.

**Tables Caption**

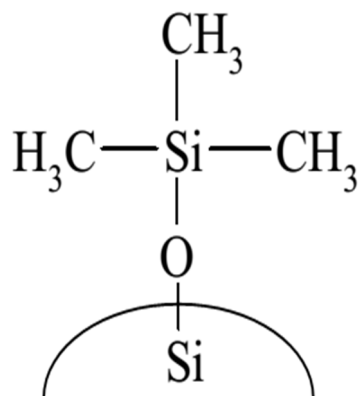
Table 1. Main findings related to binary FS-POSS nanocomposite membranes.

Table 1.

Membrane		Major findings	Ref.
PTMSP	POSS OL1160	The incorporation of 10 wt.% POSS decreased membrane permeability by 70%. The permeation was stable during the experiment (up to 27 days). This indicated that physical aging was exhibited obviously by incorporating POSS nanoparticles.	<sup>28</sup>
PTMSP	POSS MS0865	The incorporation of 10 wt.% POSS decreased membrane permeability by 55%, while the FFV and permeability were stable over time for PTMSP nanocomposite membranes having 10 wt.% POSS nanoparticles. POSS prop open the larger free volume elements of PTMSP, mitigating the physical aging by avoiding the collapse of larger free volume elements.	<sup>29, 30</sup>
PTMSP	POSS OL1160	FS and POSS nanoparticles have opposite effect on membrane permeability: FS increases while POSS dramatically decreases permeability. The gas permeability of binary FS/POSS filler system appears to be an average of the permeabilities of the respective single-filler systems. Incorporation of POSS filler appears to stop aging in PTMSP and stabilizes permeability.	<sup>31</sup>

PTMSP: poly [1-(trimethylsilyl)-1-propyne]; POSS OL1160: Octavinyl-POSS; POSS MS0865: octatrimethylsiloxy-POSS

a)



b)

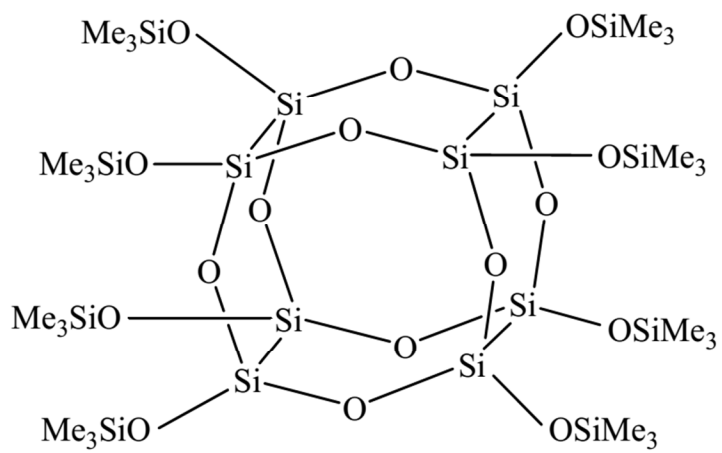


Figure 1.

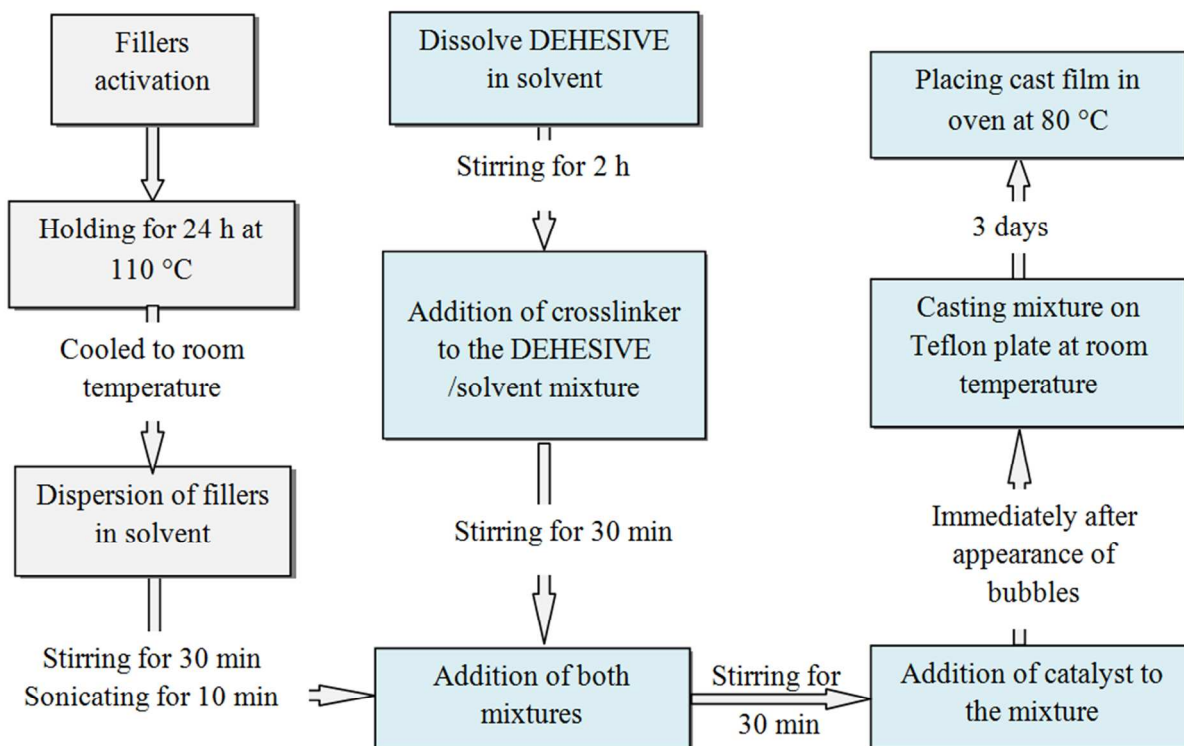


Figure 2.

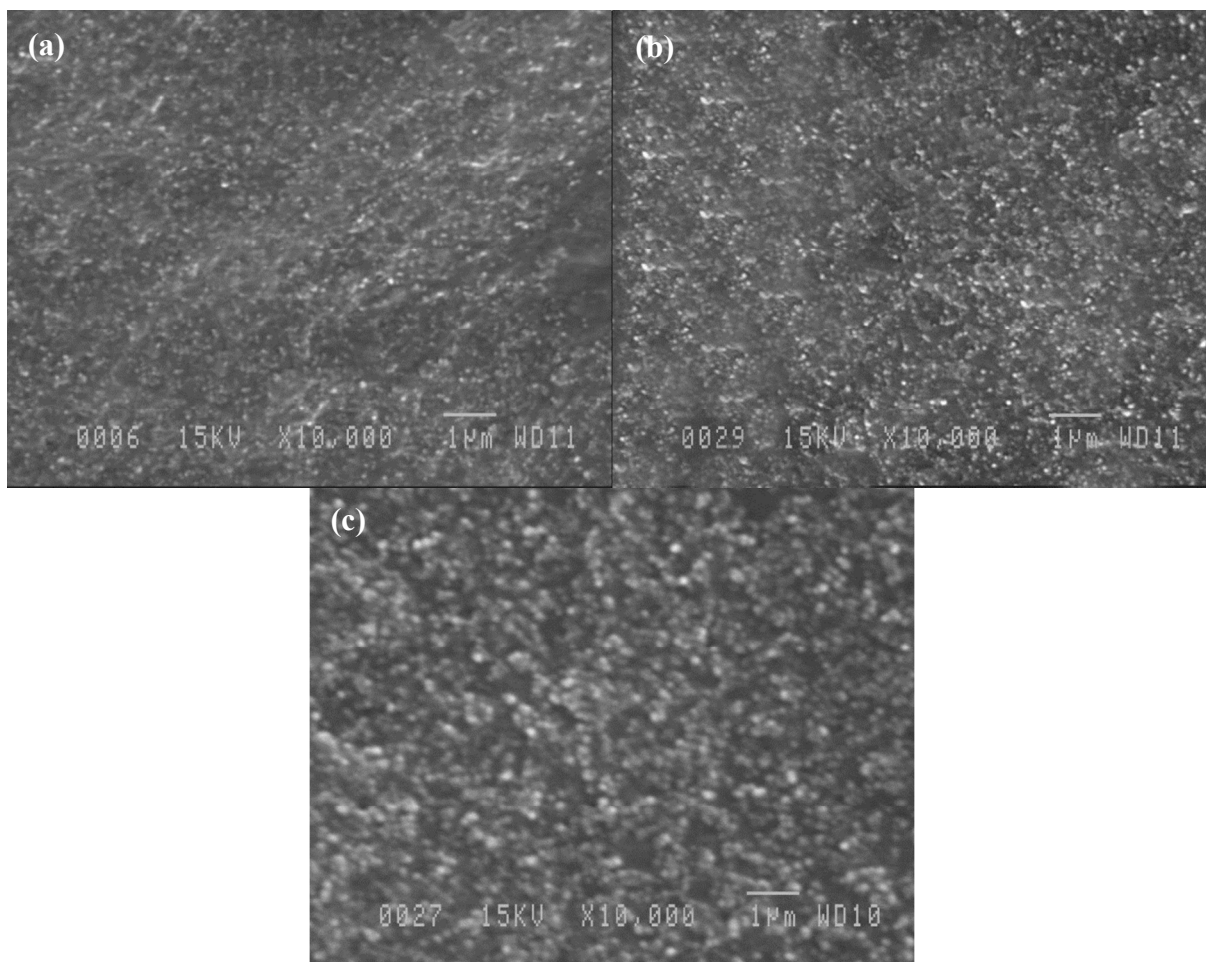


Figure 3.



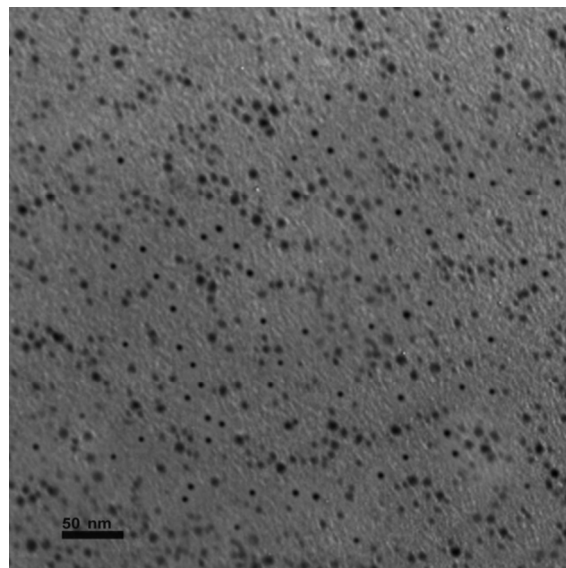


Figure 4.

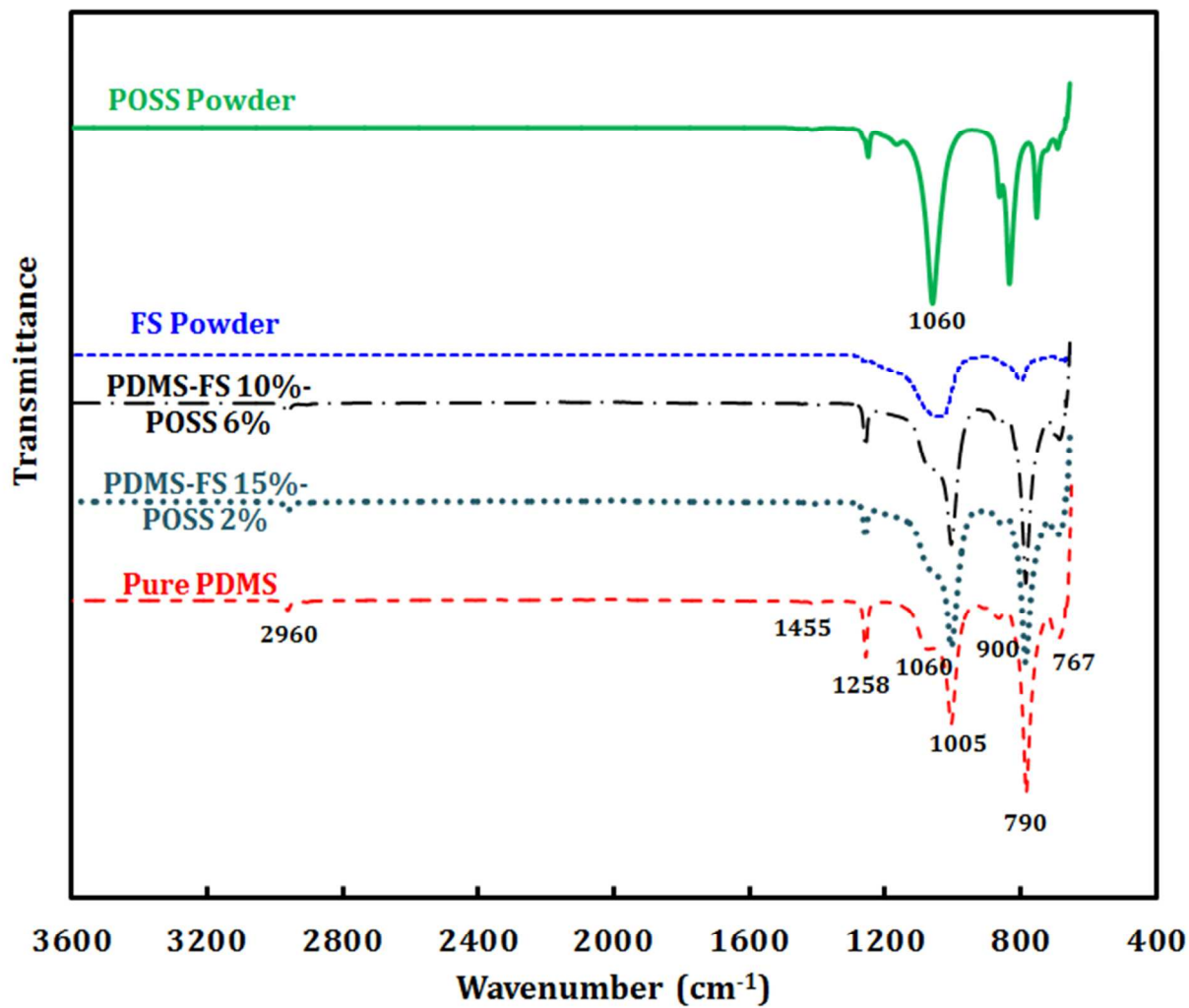


Figure 5.

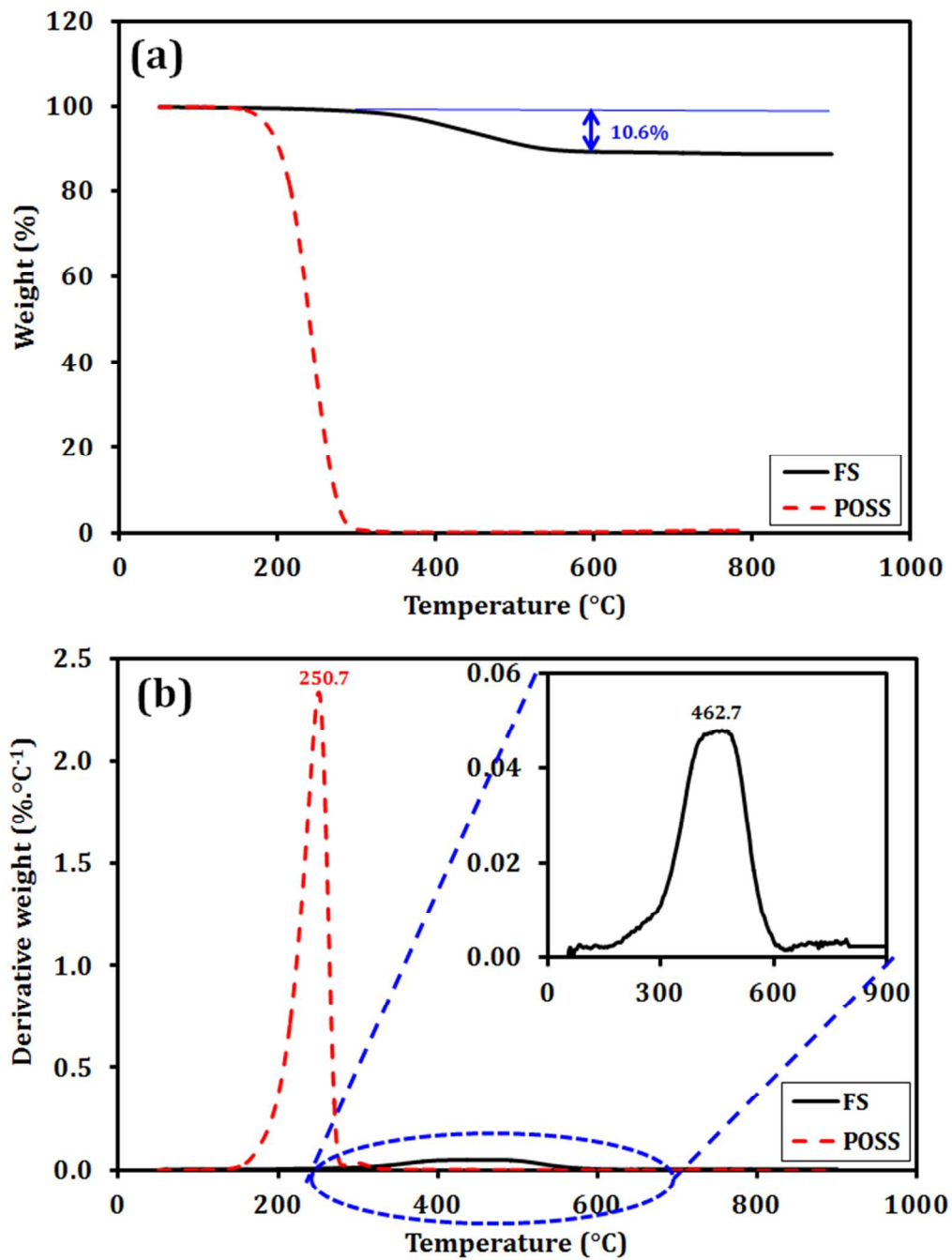


Figure 6.

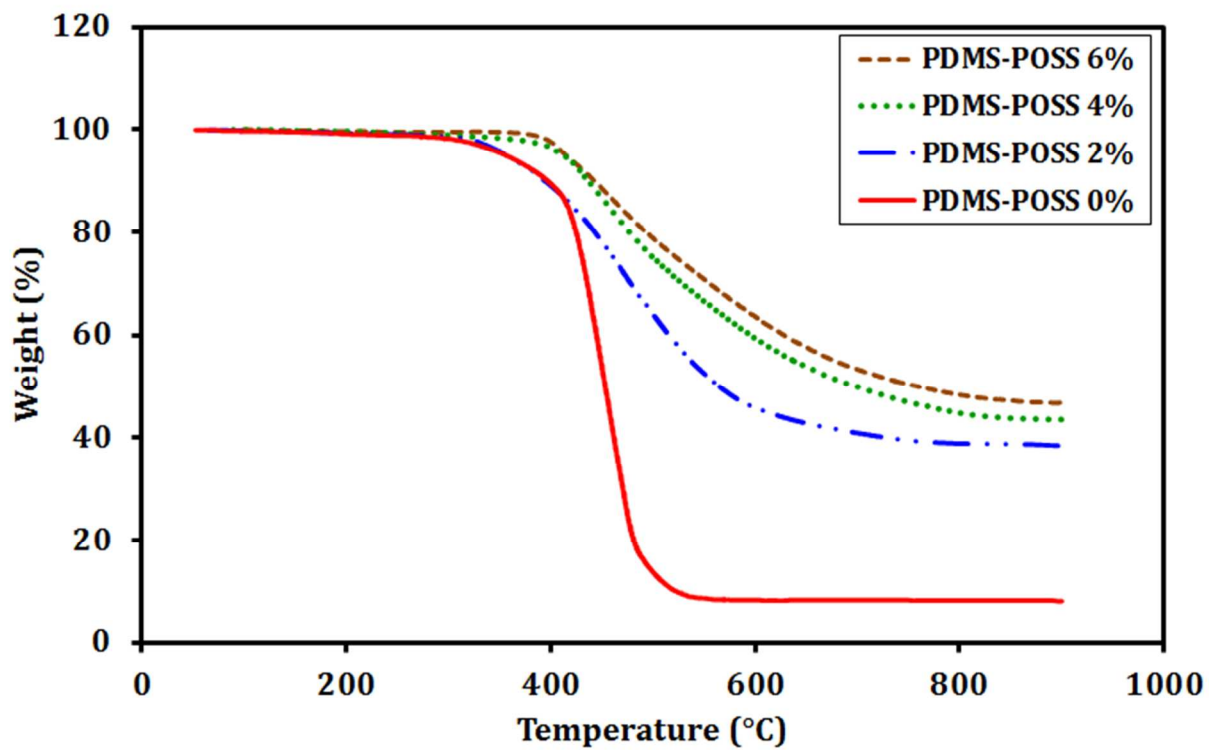


Figure 7.

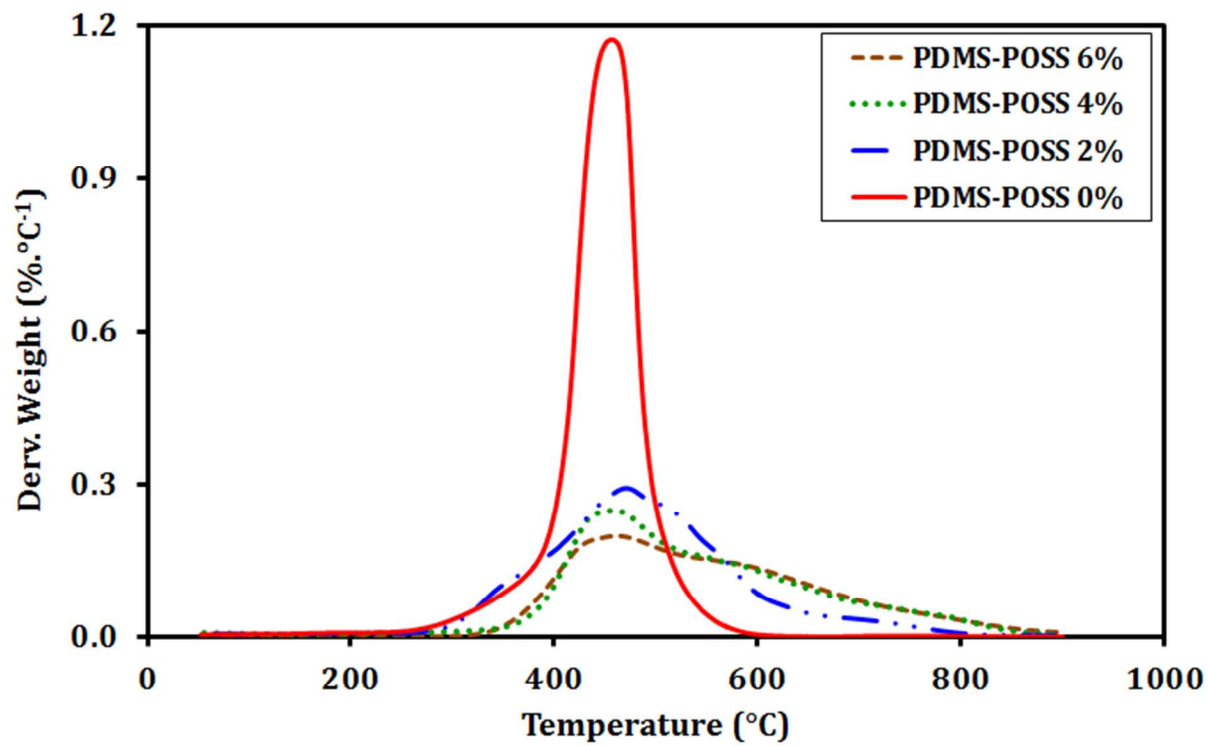


Figure 8.

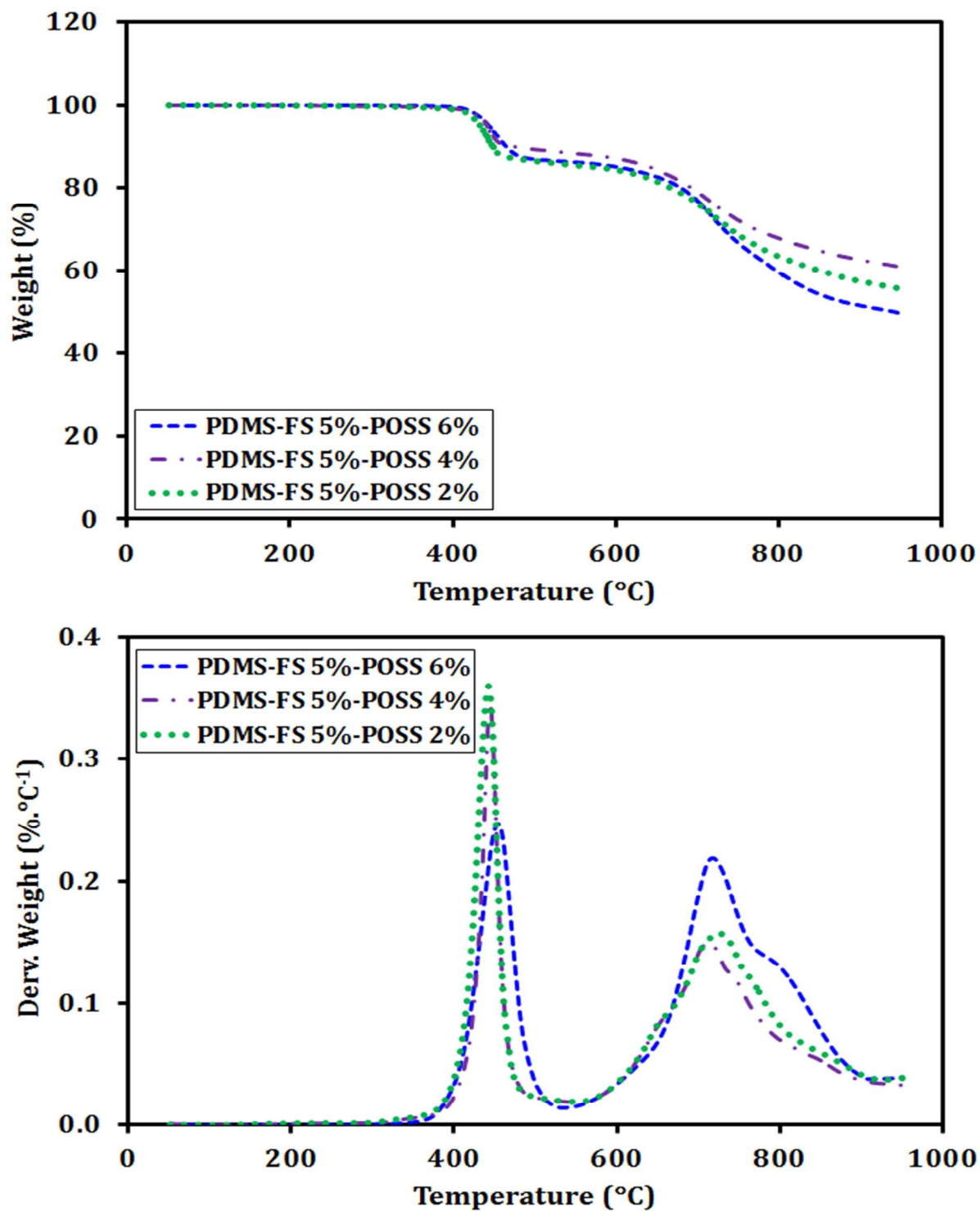


Figure 9.

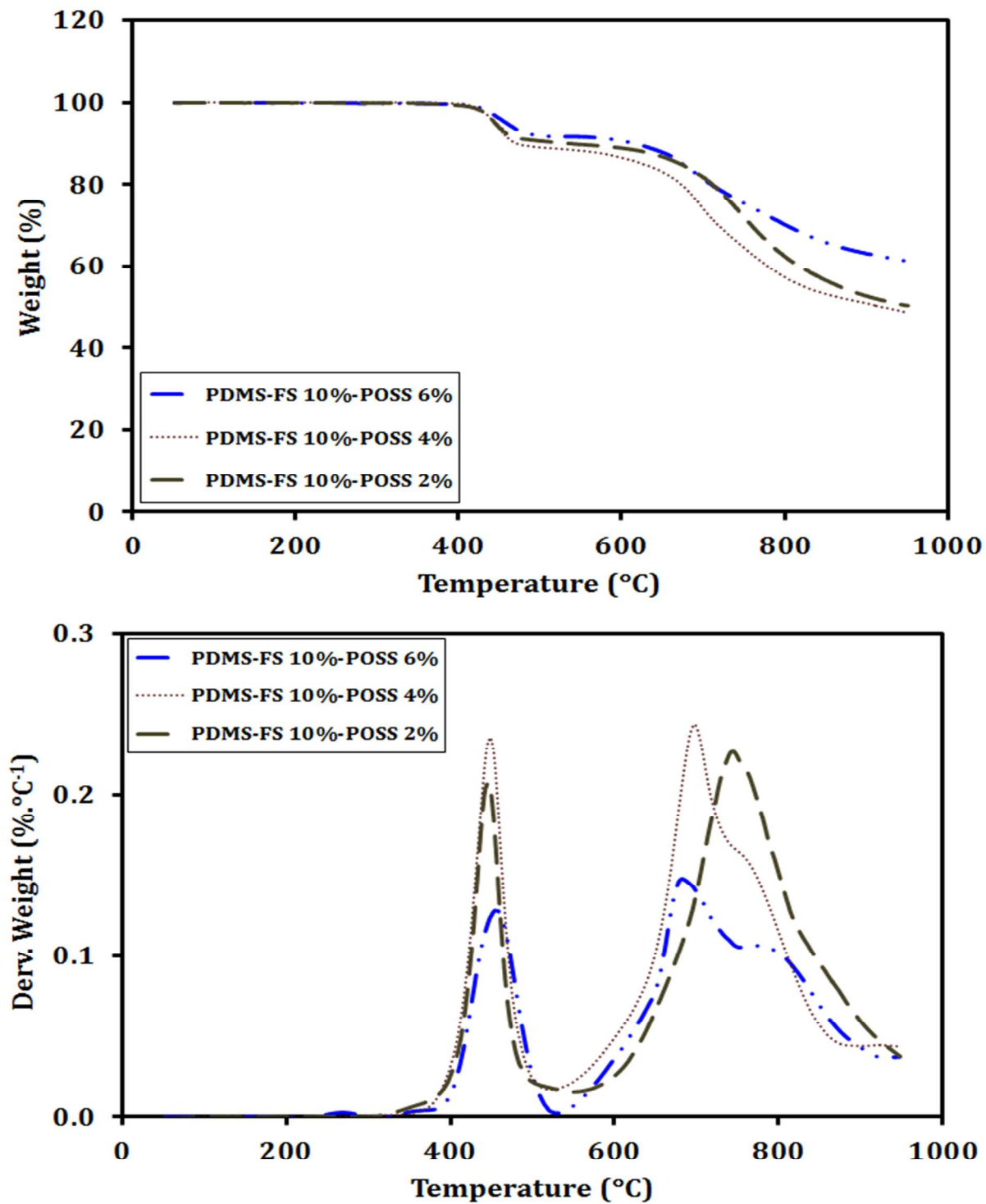


Figure 10.

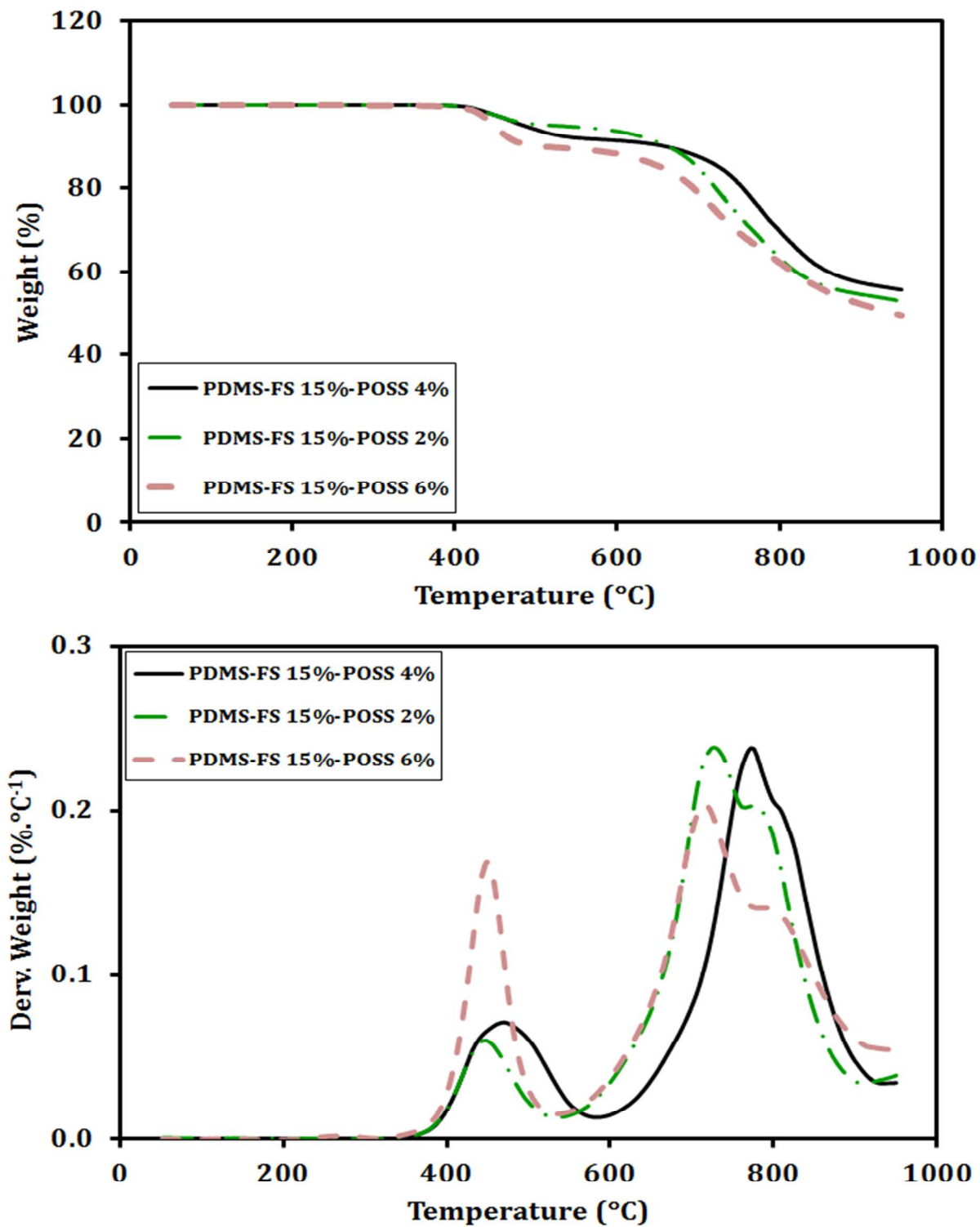


Figure 11.



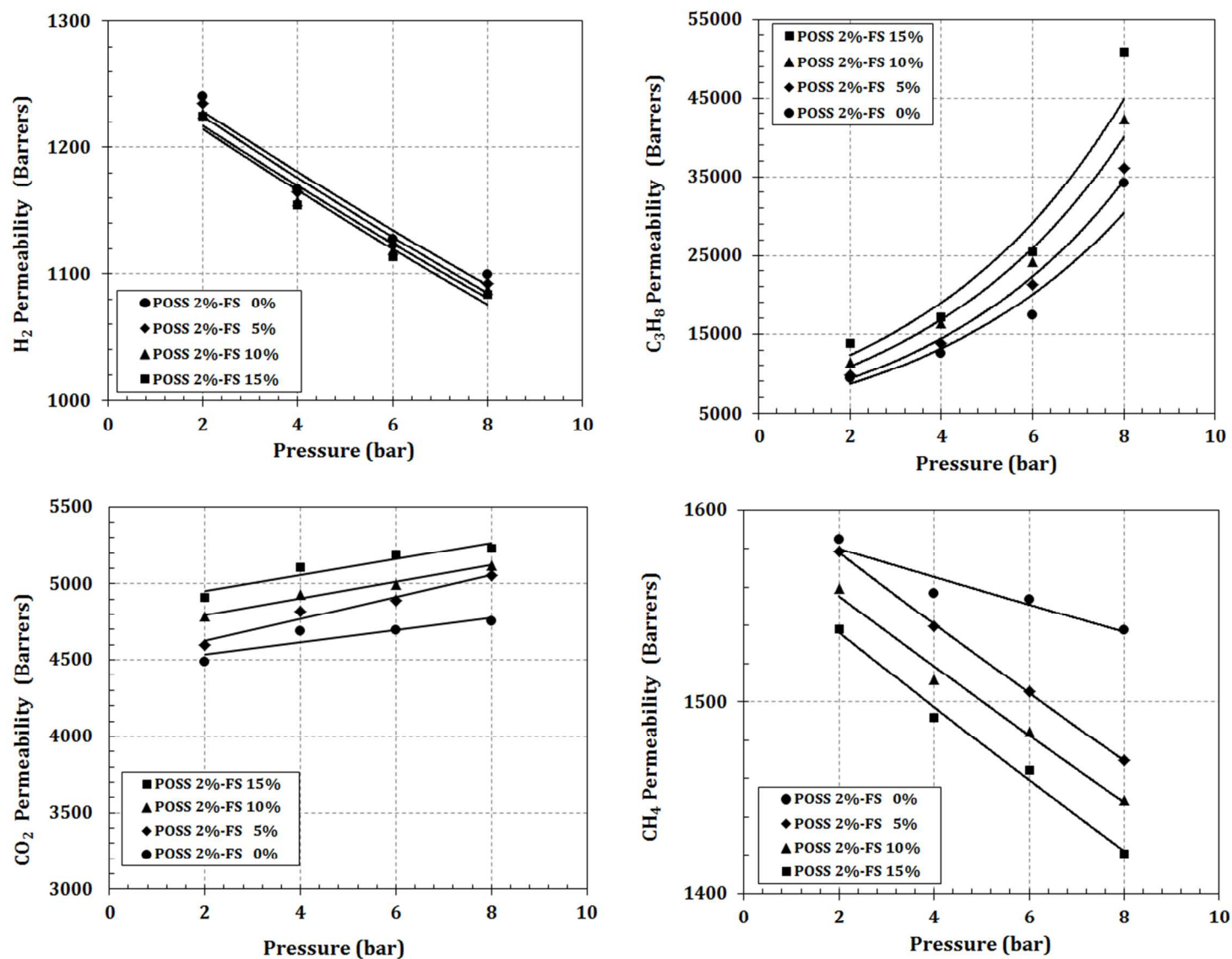


Figure 12.

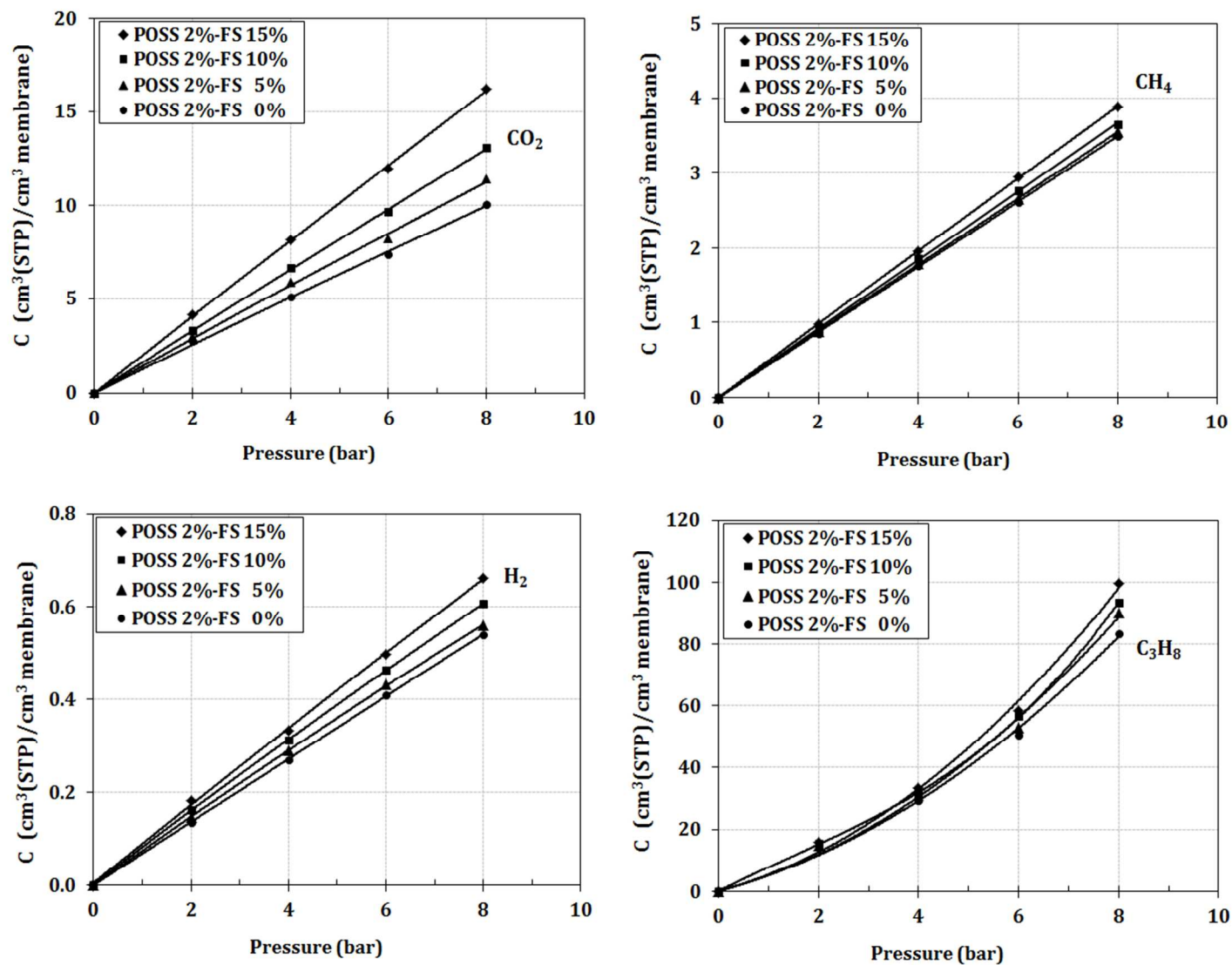


Figure 13.